1. Introduction

Alzheimer's disease (AD) is a debilitating medical condition characterised by serious and progressive cognitive decline that affects one in eight people over 65 years of age [1]. Alzheimer's disease is the most common dementia, while its precise cause (or causes) is not yet known a much explored hypothesis is that AD may be due to a failure of elimination of amyloid-β (Aβ) - a normal by-product of cell metabolism - from the brain [2, 3].

The elimination of Aβ is thought to occur via fluid flow through extracellular spaces in the brain; these spaces contain interstitial fluid (ISF) which is produced by the blood and by-products of cell metabolism. The extracellular spaces within the walls of cerebral blood vessels referred to as *basement membranes* represent the perivascular pathways along which ISF drains out of the brain [2, 3, 4].

One mechanism for the removal of Aβ from the brain parenchyma is perivascular drainage, by which Aβ within the ISF enters the capillary basement membranes, draining along the walls of arteries towards the surface of the brain [see Figure 1].

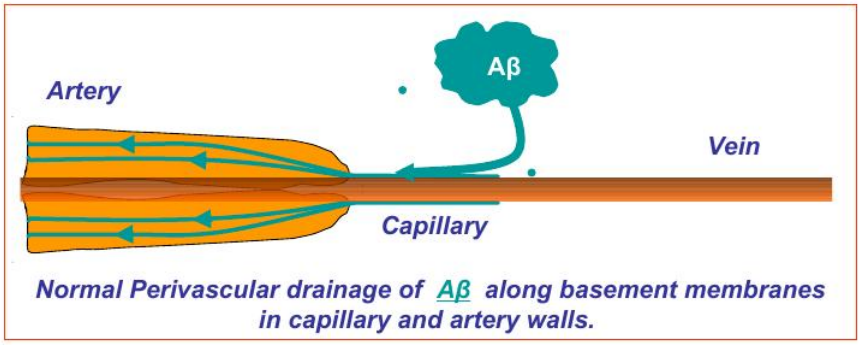

Figure 1. Perivascular drainage of Aβ along basement membranes.

With ageing and certain genetic disposition soluble Aβ is not eliminated from the brain, but instead is deposited in the walls of blood vessels as *Cerebral Amyloid Angiopathy* (CAA) [3, 4]. It is conjectured that CAA causes a blockage in the ISF drainage pathways resulting in an alteration of the composition of ISF in the brain parenchyma. This change in biochemical composition of the ISF leads to nerve cell death and Alzheimer's Disease [4].

Susceptibility to CAA varies throughout the brain and vascular vessels. In particular CAA is most prominent in the occipital, temporal and frontal lobes and least prominent in the parietal lobe and the cerebellum [5]. We suspect that one reason for the differing susceptibility of CAA is the differing symmetry of the cerebral arterial tree.

High levels of symmetry have been shown to be advantageous in other networks. For example Song *et al.* found that a fractal biochemical annotation network (a graph with a high level of symmetry) is more robust than a less symmetric biochemical annotation network [6]. In order to test the hypothesis that symmetry effects susceptibility to CAA we design and implement a graph theoretic algorithm that models CAA.

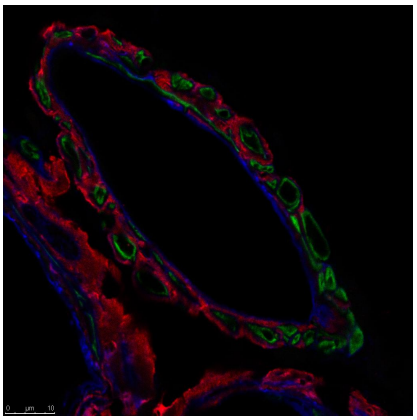

FIGURE 2. CAA in a cross-section of a leptomeningeal artery: the deposition of Aβ is shown in red. The walls of cerebral capillaries consist of one fused layer of basement membrane which is approximately 150 nm in thickness.

2. Background

In Section 3 we will describe an algorithm that models CAA. This algorithm consists of two parts; a model of the anatomical structure of the perivascular drainage system and a process that replicates the accumulation of Aβ. We will describe this model in the language of graph theory thereby reformulating CAA as a graph process.

2.1. **Graphs and Trees.**

Graph theory has a rich mathematical history dating back to Leonard Euler although more recently graph theory, under the guise of the much ballyhooed *Science of Networks*, has been applied to model biological, technological and social phenomena [7]. For the purposes of this paper we will restrict our dicussion to a particular subset of graphs called *trees*.

Trees are mathematical structures comprising of points called "vertices" and lines between them called "edges". Trees are drawn with a dot or circle for each vertex and a line between a pair of dots if there is an edge between them. More formally we write V for the set of vertices and E for the set of edges of a tree.

Each edge $e \in E$ begins and ends at distinct vertices $v, w \in V$ and we write $e = (vw)$. We say that two vertices are *adjacent* if they are connected via an edge. See Figure 3 for an example of a tree with vertices $V = \{V1, V2, V3, V4, V5\}$ and edges $E = \{(V1V2), (V2V3), (V2V4), (V2V5)\}$.

It is possible to encode more information in a tree by giving each edge a number or *weight*. For example, a tree representing a road network with vertices as junctions and edges as roads could usefully be weighted by the capacities of each road. We depict a weighted tree by writing the weight of each edge next to that edge.

It is said that it is not what you know but who you know that counts and this is especially true in the case of trees. Each vertex "knows" the vertices connected by an edge to itself. In addition, "How many you know" is a significant quantum of information given by the number of edges incident to a vertex. More formally

the degree, $\deg(v)$, of a vertex v is the number of edges incident to v. If $\deg(v) = 1$ then we say that v (and the edge incident to v) is a *leaf*.

A cycle is a is a sequence of distinct consecutive edges beginning and ending at the same vertex that doesn't visit any edge more than once. Formally a tree is a pair $T = (V, E)$ if T does not admit any cycles and there exists a sequence of distinct consecutive edges between every pair of vertices $v, w \in V$ [8].

The vascular system comprises of a hierarchy of vessels: blood flows from arteries to arterioles to capillaries. To reflect this hierarchy our model will incorporate a *rooted* tree: a tree in which one vertex has been assigned the role of *root*. The assigned root vertex in our model will correspond to the point where Aβ drains out of the cerebral vasculature and into the lymphatic system. The *level* of each vertex $v \in V$ is the number of edges in the unique sequence of distinct consecutive edges between v and the root; we write this as $\mathrm{lv}(v)$.

Given any structure such as a tree it is natural to want to define appropriate substructures. For example we might be interested in a particular subset of the cerebral arterial tree. More formally, given a tree $T = (V, E)$ and a vertex $v \in V$ the *induced subtree of* T *rooted at* v consists of vertex v, all vertices w adjacent to v such that $\mathrm{lv}(w) > lv(v)$, all vertices u adjacent to w such that $\mathrm{lv}(u) > lv(w)$ and so on, *and* all edges with endpoints in the set of vertices described above. For example, the vertices coloured blue in Figure 3 together with the edge set $\{(V2V3), (V2V4)(V2V5)\}$ is an induced subtree of T rooted at $V2$.

The appropriate graph to model any phenomenon will have properties such as a restriction on the degree of a particular or all of the vertices. For example the majority of branching in the cerebral arterial tree is bifurcation (blood flows from one larger incoming vessel into two smaller outgoing vessels) [9] so the majority of vertices in the appropriate model would have degree 3. If the degree of every vertex of a tree is 3 or less (and the degree of the root vertex is 2 or less) then we call that tree a *binary* tree ("binary" refers to the number of outgoing vessels). For example, the tree depicted in Figure 3 is *not* a binary tree since $\deg(V2) = 4$.

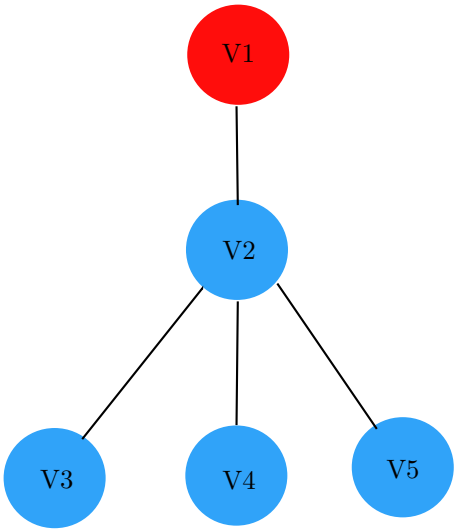

FIGURE 3. Tree, T with edges $\{(V1V2)(V2V3)(V2V4)(V2V5)\}$. We may permute edges $\{(V2V3)(V2V4)(V2V5)\}$ whilst preserving adjacent vertices in 6 possible ways so $|\mathrm{Sym}(T)| = 6$. By assigning $V1$ to be the root of T notice that $\mathrm{lv}(V1) = 0, \mathrm{lv}(V2) = 1, \mathrm{lv}(V3) = \mathrm{lv}(V4) = \mathrm{lv}(V5) = 2$.. The vertices marked in blue represent an induced subtree of T, rooted at $V2$.

One might describe an object as symmetric if it can be rotated or reflected in such a way that the object looks "the same" after the rotation or reflection. For example, if the square shown in Figure 6 is rotated by 0,90,180,270 degrees or reflected in the straight lines through opposite corners or opposite midpoints then the resulting square is indistinguishable from the original.

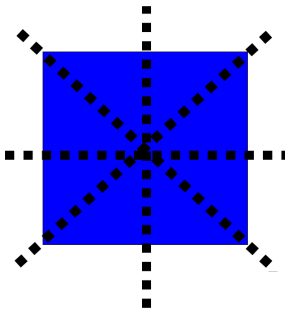

FIGURE 4. Lines of reflective symmetry for a square.

Similarly a tree can be described as symmetric if that tree looks the same after we have moved edge and vertices.

Remark. One can formally quantify the symmetry of a mathematical object such as a tree or square by identifying that object's *group of symmetries*. For example, every tree, T, can be associated with a group of symmetries, $\mathrm{Sym}(T)$, that consists

of all permutations of vertices/edges that preserves vertex adjacency. The number of possible legal permutations is written as $|\mathrm{Sym}(T)|$ and we say that a tree with a larger number of legal permutations is more *symmetric* than a tree with a smaller symmetry group.

Recall from Section 1 the hypothesis that there exists correlation between a high degree of symmetry and network robustness. To gain some intuition into this hypothesis consider the following (extreme) example. Let T_1 be the tree on 15 vertices depicted on the left and T_2 be the line of 15 vertices depicted on the right of Figure 5 [below].

These trees have the same number of vertices and edges but hugely different symmetry groups. We view each edge as a pipe and imagine that fluid flows on T_1 and T_2 through these pipes towards vertex the root vertex (labelled 1). If we remove an edge from either tree then all the edges flowing into that edge become redundant. Tree T_2 is significantly more vulnerable to attack because if we remove an edge from T_2 all the edges to the right of the removed edge are rendered useless. Whereas, if we remove an edge from T_1 we only remove the edges lower than the removed edge.

To quantify the different levels of robustness in T_1 and T_2 we wil calculate the total number of edges removed if we remove each of the 14 edges and take an average for each tree. This average is the *expected* number of edges removed.

Since $|\mathrm{Sym}(T_1)| = 128$ and that $|\mathrm{Sym}(T_2)| = 2$, T_1 is more symmetric than T_2.

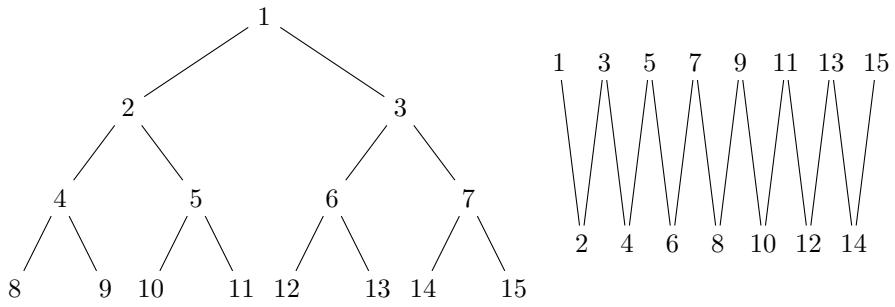

FIGURE 5. T_1 and T_2

If we remove an edge at random from T_1 and also remove the induced subtree adjacent to that edge the expected number of edges removed is:

$$1\frac{8}{14} + 3\frac{4}{14} + 7\frac{2}{14} = \frac{12}{7} \tag{1}$$

If we remove an edge at random from T_2 and also remove the induced subtree adjacent to that edge the expected number of edges removed is:

$$\frac{1}{14}\sum_{k=1}^{14} k = \frac{15}{2} > \frac{12}{7} \tag{2}$$

2.2. **Anatomical data.** In order to build an effective model of CAA we will incorporate relevant anatomical data such as arterial length, branching and the radius

of vessels [1] in our model. Cassot *et al.* conducted a detailed analysis of the cerebral vasculature which has formed the basis of numerous numerical analyses [**?**, 9]. Cassot *et al.* found that 98% of branching in the cerebral cortex is bifurcation (i.e. each non-root vertex has valence 3) and there are approximately 300 branching points (vertices) [9].

Recall from Section 1 that extracellular spaces within the walls of cerebral blood vessels are the pathways along which ISF drains from the brain. In Section 3 we will describe a model of ISF flow in which we think of cerebral arterial vessels as cylinders and these cerebral perivascular pathways as *annular prisms* surrounding arterial vessels.

At an arterial bifurcation point with parent blood vessel p and daughter blood vessels d_1 and d_2 Murray's law [11] states that:

$$r_p^3 = r_{d_1}^3 + r_{d_2}^3$$

where r_p is the radius of p and r_{d_1}, r_{d_2} are the radii of d_1 and d_2 respectively. Experimental evidence has shown that Murray's law is a good approximation for arterial vessels [10, 12]. Since Murray's law describes the relationship between bifurcating arterial vessels but we will model the cerebral perivascular pathways it is necessary to adjust Murray's law to describe the relationship between parent and child annular prisms. In addition we make the simplifying assumtion that the width, ϵ [see Figure 6], of the perivascular pathways is the same for every vessel. Since the notion of radius is more complicated for an annular prism we reformulate Murray's law in terms of cross-sectional area in Lemma 2.1.

Lemma 2.1 (Murray's law adjusted for annular prisms)**.** *Let the parent vessel have radius $r_p = r'_p + \epsilon$ and the two daughter vessels have radii $r_{d_i} = r'_{d_i} + \epsilon$ for $i = 1, 2$.*

$$A_p = \pi \left(\epsilon^2 + 2\epsilon \left(\left(\frac{A_{d_1} + \pi\epsilon^2}{2\epsilon\pi} \right)^3 + \left(\frac{A_{d_2} + \pi\epsilon^2}{2\epsilon\pi} \right)^3 \right)^{\frac{1}{3}} \right)$$

where A_p is the cross-sectional area of the parent vessel and A_{d_1} and A_{d_2} are the cross-sectional areas of the two daughter vessels at a bifurcation.

Proof. The relationship between the cross-sectional area, A_X of any vessel and the radius, r_X of that vessel is given by the formulae:

$$\begin{aligned} A_X &= \pi((r'_X + \epsilon)^2 - r'^2_X) \\ &= \pi(\epsilon^2 + 2\epsilon r'_X) \\ r'_X &= \frac{A_X - \pi\epsilon^2}{2\epsilon\pi} \\ r_X &= \frac{A_X - \pi\epsilon^2}{2\epsilon\pi} + \epsilon \\ &= \frac{A_X + \pi\epsilon^2}{2\epsilon\pi} \end{aligned}$$

By combining the above equations we find that the cross-sectional area of the parent vessel, A_p, is given by:

[1] There is a great deal of disagreement and ambiguity in the literature pertaining to arterial vessel segments and branching points [10]. We will use the definitions given by Cassot *et al.* [9]

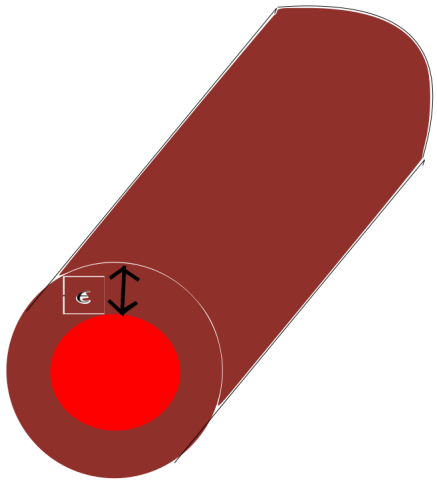

FIGURE 6. An annular prism with radius ϵ

$$\begin{aligned} A_p &= \pi(\epsilon^2 + 2\epsilon r_p) \\ &= \pi\left(\epsilon^2 + 2\epsilon(r_{d_1}^3 + r_{d_2}^3)^{\frac{1}{3}}\right) \\ &= \pi\left(\epsilon^2 + 2\epsilon\left(\left(\frac{A_{d_1} + \pi\epsilon^2}{2\epsilon\pi}\right)^3 + \left(\frac{A_{d_2} + \pi\epsilon^2}{2\epsilon\pi}\right)^3\right)^{\frac{1}{3}}\right) \end{aligned}$$

□

3. METHOD

In this section we will describe the algorithm we designed to replicate CAA [2]. This algorithm has three constituent parts:

(i) Generate 50 random rooted trees; $\mathcal{T} = \{T_1, T_2, \ldots, T_{50}\}$.
(ii) Calculate the order of the symmetry group of each tree using the graph isomorphism program *nauty* [14].
(iii) Replicate CAA by randomly removing edges.

Each tree encodes the anatomical information discussed in Section 2.2. Graphical characteristics of each tree such as the degree of each vertex were determined by the anatomical survey of cerebral vascular trees carried out by Cassot *et al.* [9]. As we are modelling perivascular drainage rather than blood flow each branch

[2]This algorithm was implemented using the numerical modelling program *matlab* [13]

was assigned a number representing the total volume of the basement membrane enveloping the relevant arterial tree.

For each randomly generated tree T_i let $E(T_i)$ be the set of edges of T_i and $V(T_i)$ be the set of vertices of T_i. Each rooted binary tree was generated with 300 vertices and every edge $e \in E(T_i)$ was associated with an annular prism and assigned a volume $\mathrm{vol}(e)$. Leaf edges were defined to have volume 1 and subsequent edges were given a volume consistent with Murray's law for annular prisms (see Lemma 2.1). Each non-root vertex had maximum valence 3 and each root vertex had maximum valence 2.

The fundamental assumption we made when we replicated CAA was that it is more likely for an edge to succumb to CAA if the concentration of Aβ in that edge is higher. Since the production of Aβ is approximately constant throughout a human lifetime [3] we assumed that the rate of removal of $A\beta$ into the lymphatic system (the root vertex in our model) was constant. This implies that when a vascular unit becomes blocked via CAA the concentration of Aβ in the intact perivascular pathways increases forming a devastating negative feedback loop. Our model incorporated these assumptions by calculating the concentration of Aβ in terms of the functioning part of the weighted, rooted , binary tree.

The *initial* volume of each tree T_i was defined to be

$$\mathrm{Vol}(T_i) = \sum_{e \in E(T_i)} \mathrm{vol}(e)$$

The process of edge removal proceeds as follows: at time $t = 0$ we set $T_i(0) = T_i$ (our randomly generated rooted binary tree). At subsequent times $t = 1, 2, \ldots$ we uniformly associated a probability $0 < P_t \leq 1$, with every edge such that for each edge the probability that it was removed was P_t. The removal of an edge from T_i represented a blockage in the perivascular system. Such a blockage in the basement membrane results in a failure of drainage from all vessels that feed that edge. Therefore, if edge (vw) was removed and (without loss of generality) $\mathrm{lv}(v) < \mathrm{lv}(w)$ then we also removed the induced subtree rooted at w from $T_i(t-1)$.

The volume of T_i at time t was defined to be $\mathrm{Vol}_t(T_i) = \sum_{e \in E(T_i(t))} \mathrm{vol}(e)$. We then defined concentration:

$$C(t) = \frac{\mathrm{Vol}(T_i)}{\mathrm{Vol}_t(T_i)}.$$

We can now define

$$P_t = \begin{cases} p.C(t) & \text{if } p.C(t) < 1 \\ 1 & \text{otherwise} \end{cases} \quad \text{where } 0 < p < 1$$

Finally, we recorded the time, τ_i, taken to remove half of the edges from each tree T_i (henceforth we will refer to τ_i as the *half-life*).

4. Results

For each tree T_i we calculated the order of the symmetry group $|\mathrm{Sym}(T_i)|$ and the minimum time, τ_i, taken for at least half of the edges $e \in E(T_i)$ to be removed from T_i. We further calculated the median order of symmetry group, $\phi =$, and partitioned $\mathcal{T}$ into two subsets as follows:

$$\mathcal{T}_1 = \{T_i \in \mathcal{T} : |\mathrm{Sym}(T_i)| < \phi\} \text{ and } \mathcal{T}_2 = \{T_i \in \mathcal{T} : |\mathrm{Sym}(T_i)| \geq \phi\}$$

We also calculated the mean values, μ_j $(j = 1, 2)$ of τ_i for trees in $\mathcal{T}_j$ for $j = 1, 2$:

$$\mu_j = \frac{\sum_{T_i \in \mathcal{T}_j}}{|\mathcal{T}_j|}$$

Figure 7 shows the μ_j corresponding to the $\mathcal{T}_j$

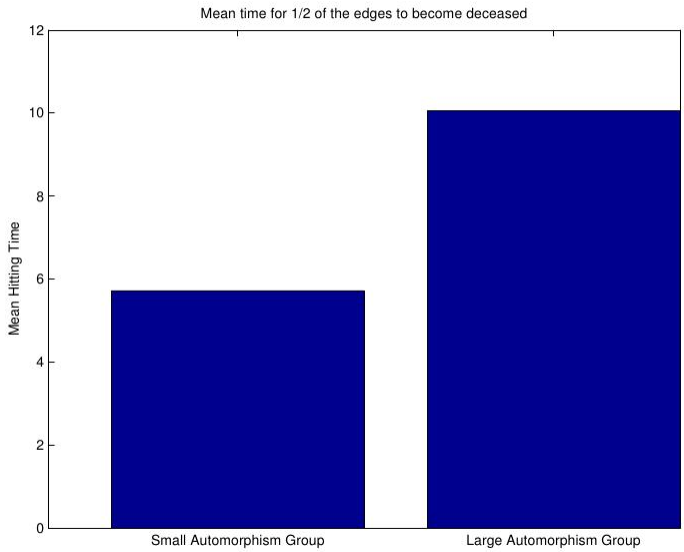

FIGURE 7. Mean time for $\frac{1}{2}$ edges to be removed for high and low values of $|\operatorname{Sym}(T_i)|$

It is clear that in general the trees with a larger symmetry group had a greater half-life.

5. Discussion

In order to place our results back into a medical context recall that the edges and vertices of each tree T_i correspond to arterial vessels and branching points respectively. The half-life, τ_i associated with each tree describes the rate at which drainage pathways become obstructed i.e. the rapidity of the onset of CAA.

In order to build an effective model of CAA it was necessary to make several simplifying assumptions. We defined the probability that an edge was removed in terms of the concentration of Aβ but the distribution of deposition of Aβ in a real arterial vessel is complex and not yet fully understood Further, our model of CAA was discrete, i.e. an edge either allowed free flow of ISF or was blocked but in reality CAA is a gradual process. We would recommend the inclusion of variable edge flow to build a more sophisticated model of CAA.

Ambrose has shown that the brain undergoes angiogenisis which could be reflected by including a new random parameter which governs the introduction of edges in our algorithm [**?**]. Modelling basement membranes as annular prisms does

not take into account the tortuous routes of perivascular drainage therefore one might also include a tortuosity parameter in a more refined model. Finally, we could model arteriosclerosis (suspected to be a major contributing factor to CAA [3]) by introducing a monotonically decreasing radial function.

Our results suggest that a more symmetric cerebral arterial tree could indicate a higher degree of robustness to CAA, however we stress that ours is a very rudimentary model. Further evidence of this correlation could be found by experiment examining the relationship between highly symmetric areas of the brain and the extent to which those areas are affected by CAA.

6. Conclusion and Clinical Implications

We have demonstrated that it is likely that there is correlation between symmetry of the cerebral vasculartureand lower risk of proliferation of CAA.

References

[1] F. Mangialasche *et al.*, Lancet neurology **9**, 702 (2010).
[2] R. O. Weller, D. Boche, and J. A. Nicoll, Acta neuropathologica **118**, 87 (2009).
[3] R. O. Weller, M. Subash, S. Preston, I. Mazanti, and R. Carare, Brain Pathology **18**, 253 (2008).
[4] D. Schley, R. Carare-Nnadi, C. Please, V. Perry, and R. Weller, Journal of Theoretical Biology **238**, 962 (2006).
[5] S. Preston, P. Steart, A. Wilkinson, J. Nicoll, and R. Weller, Neuropathology & Applied Neurobiology **29**, 106 (2003).
[6] C. Song, S. Havlin, and H. A. Makse, Nature Physics **2**, 275 (2006).
[7] H. Jeong, B. Tombor, R. Albert, Z. N. Oltvai, and A.-L. Barabási, Nature **407**, 651 (2000).
[8] B. Bollobás*Modern graph theory* Vol. 184 (Springer Verlag, 1998).
[9] F. CASSOT, F. LAUWERS, C. FOUARD, S. PROHASKA, and V. LAUWERS-CANCES, Microcirculation **13**, 1 (2006).
[10] M. Zamir, The Journal of General Physiology **67**, 213 (1976), http://jgp.rupress.org/content/67/2/213.full.pdf+html.
[11] C. D. Murray, The physiological principle of minimum work: I. the vascular system and the cost of blood volume., 1926.
[12]
[13] *MATLAB* (The MathWorks Inc., Natick, Massachusetts, 2010).
[14] *nauty* .